AD-A190 599 THE CRREL (COLD REGIONS RESEARCH AND ENGINEERING LABORATORY) HOPKINSON BAR APPARATUS(U) COLD REGIONS RESEARCH AND ENGINEERING LAB HANOVER NH 1/1

UNCLASSIFIED P K DUTTA ET AL DEC 87 CRREL-SR-87-24 F/G 11/7 NL

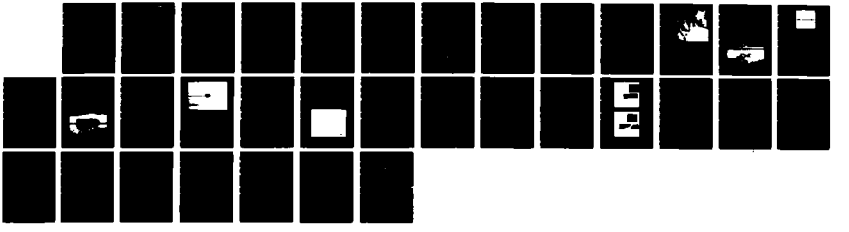

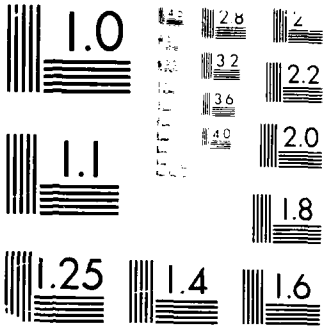

MICROCOPY RESOLUTION TEST CHART

(4)

Special Report 87-24

December 1987

US Army Corps
of Engineers
Cold Regions Research &
Engineering Laboratory

The CRREL Hopkinson bar apparatus

Piyush K. Dutta, Dennis Farrell, and John Kalafut

Prepared for
OFFICE OF THE CHIEF OF ENGINEERS

88 3 14 138

UNCLASSIFIED
SECURITY CLASSIFICATION OF THIS PAGE

REPORT DOCUMENTATION PAGE

Form Approved
OMB No 0704 0188
Exp Date Jun 30 1986

1a REPORT SECURITY CLASSIFICATION Unclassified	1b RESTRICTIVE MARKINGS
2a SECURITY CLASSIFICATION AUTHORITY	3 DISTRIBUTION/AVAILABILITY OF REPORT Approved for public release; distribution is unlimited.
2b DECLASSIFICATION/DOWNGRADING SCHEDULE	
4 PERFORMING ORGANIZATION REPORT NUMBER(S) Special Report 87-24	5 MONITORING ORGANIZATION REPORT NUMBER(S)
6a NAME OF PERFORMING ORGANIZATION U.S. Army Cold Regions Research and Engineering Laboratory 6b OFFICE SYMBOL (If applicable) CECRL	7a NAME OF MONITORING ORGANIZATION Office of the Chief of Engineers
6c ADDRESS (City, State, and ZIP Code) 72 Lyme Road Hanover, New Hampshire 03755-1290	7b ADDRESS (City, State, and ZIP Code) Washington, D.C. 20314-1000
8a NAME OF FUNDING/SPONSORING ORGANIZATION 8b OFFICE SYMBOL (If applicable)	9 PROCUREMENT INSTRUMENT IDENTIFICATION NUMBER
8c ADDRESS (City, State, and ZIP Code)	10 SOURCE OF FUNDING NUMBERS PROGRAM ELEMENT NO: 6.27.30A PROJECT NO: 4A7627 30AT42 TASK NO: SS WORK UNIT ACCESSION NO: 019

11 TITLE (Include Security Classification)

The CRREL Hopkinson Bar Apparatus

12 PERSONAL AUTHOR(S)
Dutta, Piyush K., Farrell, Dennis and Kalafut, John

13a TYPE OF REPORT	13b TIME COVERED	14 DATE OF REPORT (Year, Month, Day)	15 PAGE COUNT
	FROM _____ TO _____	December 1987	33

16 SUPPLEMENTARY NOTATION

17 COSATI CODES		
FIELD	GROUP	SUB-GROUP

18 SUBJECT TERMS (Continue on reverse if necessary and identify by block number)
Dynamic strain, Hopkinson bar, Impact, Pressure bar, Strain rate, Strain wave, stress wave

19 ABSTRACT (Continue on reverse if necessary and identify by block number)

Most materials at low temperatures change their modulus and tend to become brittle. When using these materials in structural components that are likely to be subjected to impact it is important to understand their behavior at low temperatures under dynamic loading. The CRREL split Hopkinson Test Bar was designed and set up to conduct compressive strain rate tests (up to 1000 strains/s, i.e., in./in. per s) at low temperatures (down to -100°C). The results provide dynamic stress-strain relationships of materials at low temperatures by considering the transmission of the stress wave through a test specimen sandwiched between two elastic bars. The specimen is contained in a liquid-nitrogen-operated cooling environment. During the test an elastic striker impacts the bar; as a result a stress wave passes down the bar. At the specimen a part of the wave is reflected and the rest is transmitted to the second bar. Strain gauges mounted on the bars record the wave shapes, which are analyzed to obtain the dynamic stress-strain relationships. The test bars are 1-1/2 in. in diameter and each is 8 ft long. The apparatus is suitable for testing light metals, plastics, composites, rocks, ice, and frozen soil. The data acquisition and analysis system are completely automatic, using software developed at CRREL, so the system provides for a rapid and low-cost method for high strain rate behavior studies of materials.

20 DISTRIBUTION/AVAILABILITY OF ABSTRACT	21 ABSTRACT SECURITY CLASSIFICATION
☒ UNCLASSIFIED/UNLIMITED ☐ SAME AS RPT ☐ DTIC USERS	Unclassified
22a NAME OF RESPONSIBLE INDIVIDUAL Dutta, Piyush K.	22b TELEPHONE (Include Area Code) 603-646-4100 22c OFFICE SYMBOL CECRL-EA

DD FORM 1473, 84 MAR 83 APR edition may be used until exhausted
All other editions are obsolete

SECURITY CLASSIFICATION OF THIS PAGE
UNCLASSIFIED

PREFACE

This report was prepared by Dr. Piyush K. Dutta, Materials Research Engineer, and Dennis Farrell, Mechanical Engineer, of the Applied Research Branch, Experimental Engineering Division, and John Kalafut, Electronics Engineer, of the Engineering and Measurement Services Branch, Technical Services Division, U.S. Army Cold Regions Research and Engineering Laboratory. Funding for this project was provided by DA Project 4A762730AT42, Design, Construction, and Operations Technology for Cold Regions, Task SS, Combat Service Support, Work Unit 019, Behavior of Materials at Low Temperatures.

The authors express their appreciation to Dr. Malcolm Mellor for his ideas and suggestions on developing and installing the test facility and for reviewing the report. They thank Darryl Calkins, Dr. Ronald Liston, and Dr. Eugene Marvin for their encouragement. They also thank Dr. Gordon Cox for reviewing the report and making constructive suggestions. Special thanks are given to Robert Bigl who helped build the test system.

The contents of this report are not to be used for advertising or promotional purposes. Citation of brand names does not constitute an official endorsement of the use of such commercial products.

CONTENTS

ILLUSTRATIONS

THE CRREL HOPKINSON BAR APPARATUS

Piyush K. Dutta, Dennis Farrell and John Kalafut

INTRODUCTION

The safe design of structures at low temperatures must consider the brittle behavior of material under dynamic loads. In cold regions, numerous modes of dynamic loading on structures are encountered: wave action, wind action, ice movement and impact, drilling and machinery vibrations, vehicular motion, pile driving, blasting, and earthquakes are but a few examples. The hulls of ice-breaking vessels are subjected to repeated impact loading by ice. Therefore, sound engineering design for cold regions must consider material property data determined at low temperature and at high strain-rate loading. The CRREL Hopkinson bar apparatus (HBA) has been designed to perform such high strain-rate loading tests. This report describes the design and operational procedures of this apparatus and the technique used to analyze the data. In this technique, deformation characteristics of materials at high rates (50 to 1000 strains per second) are obtained by analyzing the stress waves through a test specimen sandwiched between two elastic bars.

To illustrate the capability of the testing method some experimental results are given.

BACKGROUND

The name of the Hopkinson bar originates from the work of the British physicist B. Hopkinson (1914), who carried out impact tests on various materials. In his tests he generated compressive stress pulses in long bars by impacting them on end with bullets. The compressive pulse is reflected at the opposite free end of the bar as a tensile stress pulse, and brittle materials such as rock or concrete fracture in tension under the influence of this tension pulse. Kolsky (1949, 1953) first used the idea of stress wave propagation from one bar to another through a test material sandwiched between the two bars and thus gave the method wider

applications. This method, now called the split Hopkinson bar, involves the determination of dynamic stresses, strains, or displacements occurring at the end of a bar by various sensors monitored some distance away. The documentation of the apparatus, instrumentation, and analysis is quoted frequently in the literature (Lindholm 1964, Zukas et al. 1982).

In the conventional configuration, the apparatus is used mostly for compression tests. However, various researchers have modified the apparatus to conduct tensile tests (Harding et al. 1960, Hauser 1966, Lindholm and Yeakley 1968, Christman et al. 1971, Nicholas 1981, Harding 1983, Ross et al. 1984). Duffy et al. (1971) described using the split Hopkinson bar to achieve high strain rate in torsional loading. The primary advantage of the torsional mode of wave propagation is its nondispersiveness. In addition, the radial inertia effects are not present. Nicholas (1975) extended the technique to conduct a dynamic three-point bend test (Charpy impact test) using a single bar instrumented with a strain gauge. Klepaczko (1980) has suggested the use of the Hopkinson bar method to study the dynamic fracture-initiation properties of materials. He used a wedge-loaded specimen in a conventional split Hopkinson bar arrangement to obtain dynamic load-displacement data.

THEORY OF OPERATION

A schematic of the CRREL Hopkinson bar used for compressive testing is shown in Figure 1. The striker, driven by compressed air, approaches from the left and impacts the incident bar. This sets up a compressive stress

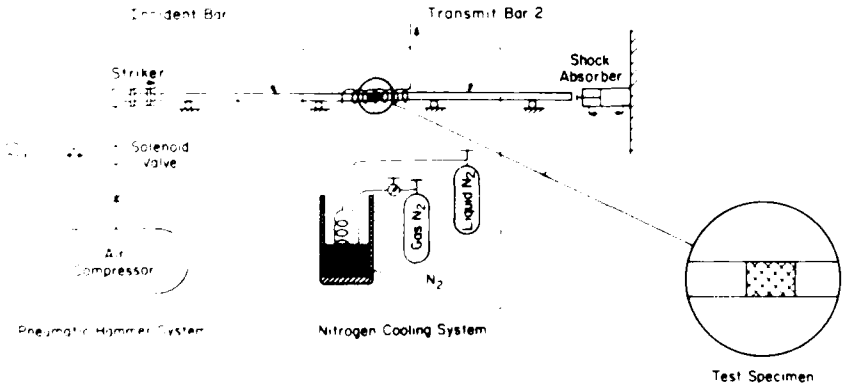

Figure 1. Split Hopkinson pressure bar system schematic.

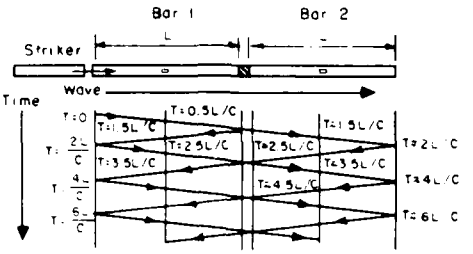

Figure 2. Lagrangian x-t diagram of stress pulse wave propagation in split Hopkinson pressure bar.

wave pulse in the incident bar. The amplitude of the stress pulse depends on the impact velocity, and the duration depends on the length and material characteristics of the striker and the incident bar. The compressive stress-wave pulse propagates through the incident bar and arrives at the incident bar/specimen interface. The details of the wave propagation in the bars are illustrated with the Lagrangian x-t diagram shown in Figure 2. At the incident bar/specimen interface, part of the incident pulse is reflected because of the mismatch of the mechanical impedances of bar and specimen. The rest is transmitted into the specimen, propagates through it, and reaches the specimen/transmitter bar interface. At this second interface, part of the stress pulse is also reflected back into the specimen and the remainder is transmitted to the transmitter bar. If the specimen is short, the wave-transmitting time will be small compared with the duration of the loading stress pulse. Thus, many wave reflections take place within the specimen during a single pulse reflection, so stress and strain along the specimen can be assumed to be uniform.

Consideration of equilibrium at the interface between specimen and transmitter bar shows that the force in the specimen and in the transmitter bar is equal. The force is measured by measuring the strain on the elastic transmitter bar using strain gauges. At the location of the strain gauge this force will have a time shift represented by the travel times from the interface.

The average strain ε_s in the specimen is calculated from the displacements at the end of the specimen. The theory is well documented (Zukas et al. 1982), and it is summarized in Appendix A for both short and

long specimens. For short specimens the analysis presented in Appendix A shows:

$$\text{specimen strain} \qquad \varepsilon_s(t) = \frac{-2c}{L_s} \int_0^t \varepsilon_r(t)dt \tag{1}$$

$$\text{specimen strain rate} \qquad \frac{d\varepsilon_s(t)}{dt} = \dot{\varepsilon}_s = \frac{-2c}{L_s} \varepsilon_r(t), \text{ and} \tag{2}$$

$$\text{specimen stress} \qquad \sigma_s(t) = E_b \varepsilon_t(t) \tag{3}$$

where

c = wave propagation velocity in the Hopkinson bars

L_s = length of specimen

$\varepsilon_r(t)$ = instantaneous reflected strain

$\varepsilon_t(t)$ = instantaneous transmitted strain

E_b = elastic modulus of the bar material.

Equation 1 shows that the average strain in the specimen can be computed by measuring the reflected strain in the incident bar. This is made possible by locating the strain gauge a sufficient distance from the interface. This allows the incident stress pulse to pass through this strain gauge station completely before the arrival of the reflected pulse from the interface. Thus, a longer pulse requires a correspondingly longer incident bar. A longer pulse is desirable because, as mentioned earlier, the strain uniformity within the specimen under repeated reflection can be ensured. Therefore longer bars, within practical limits, are more convenient and provide more accurate measurements than shorter bars.

Equation 2 shows that for high strain rate the reflected wave ε_r should be large or the specimen short. Note also that a larger reflection happens only when there is a larger mismatch in impedance* between the bar and the specimen. This occurs only when the specimen is of smaller diameter than the bar or the bar is stiffer and of higher density than the specimen material.

Areas of cross section (A), modulus of elasticity (E), and density (ρ) are the parameters that control the impedance. For example, the impedance I_A of body A matches the impedance of body B if $I_A = I_B$, i.e.

$$A_A (E_A \rho_A)^{0.5} = A_B (E_B \rho_B)^{0.5} .$$

* Mechanical impedance of an interface between two longitudinal bodies determines the wave propagation characteristics through that interface.

If $I_A > I_B$, a compressive stress wave reflects back as a tensile wave from the interface, whereas if $I_A < I_B$ a compressive stress wave reflects back as a compressive wave and vice versa.

Testing of crystalline or granular materials usually requires that specimens be 5 to 10 times (preferably 10 to 20 times) the maximum grain or crack size. Thus larger-diameter specimens are preferable. Again the diameter-to-length ratio (2:4) makes the specimens in these categories of materials longer than the metal specimens tested in the Hopkinson bars. Another disadvantage of granular material is the comparatively lower wave velocity within the specimen. Thus, for a relatively short incident wavelength, the number of internal reflections within the specimen is not large enough to make it reach a state of uniform stress. Under such conditions longer incident wavelength, and therefore longer incident bars, are desirable.

With the electronic recording and computational devices available, it is possible to record digitally all three waves (i.e. incident, reflected, and transmitted wave), superimpose them one over the other, and analyze the displacements of the two interfaces of the specimen. The average stress and strain of the longer samples can be computed as shown below (refer to Appendix A for derivation of these formulas):

average specimen strain
$$\varepsilon_s(t) = \frac{1}{\rho c L_s} \int_0^t [\sigma_i(t) - \sigma_r(t) - \sigma_t(t)]dt \quad (4)$$

average specimen strain rate
$$\dot{\varepsilon}_s = \frac{1}{\rho c L_s} [\sigma_i(t) - \sigma_r(t) - \sigma_t(t)] \text{ , and} \quad (5)$$

average specimen stress
$$\sigma_s(t) = \frac{1}{2} [\sigma_i(t) + \sigma_r(t) + \sigma_t(t)] \quad (6)$$

It is obvious that the above approach, to study the dynamic properties of materials, is indirect. The strain rates that occur during the test are primarily a function of the test material's own constitutive behavior. It is also important to note that the stress, strain, and strain rate are average values and are calculated on the basis of the uniaxial stress-state assumptions.

DESIGN DETAILS

The Hopkinson bar apparatus (Fig. 3) installed at CRREL includes three major subsystems: the stress generating system, the specimen cooling

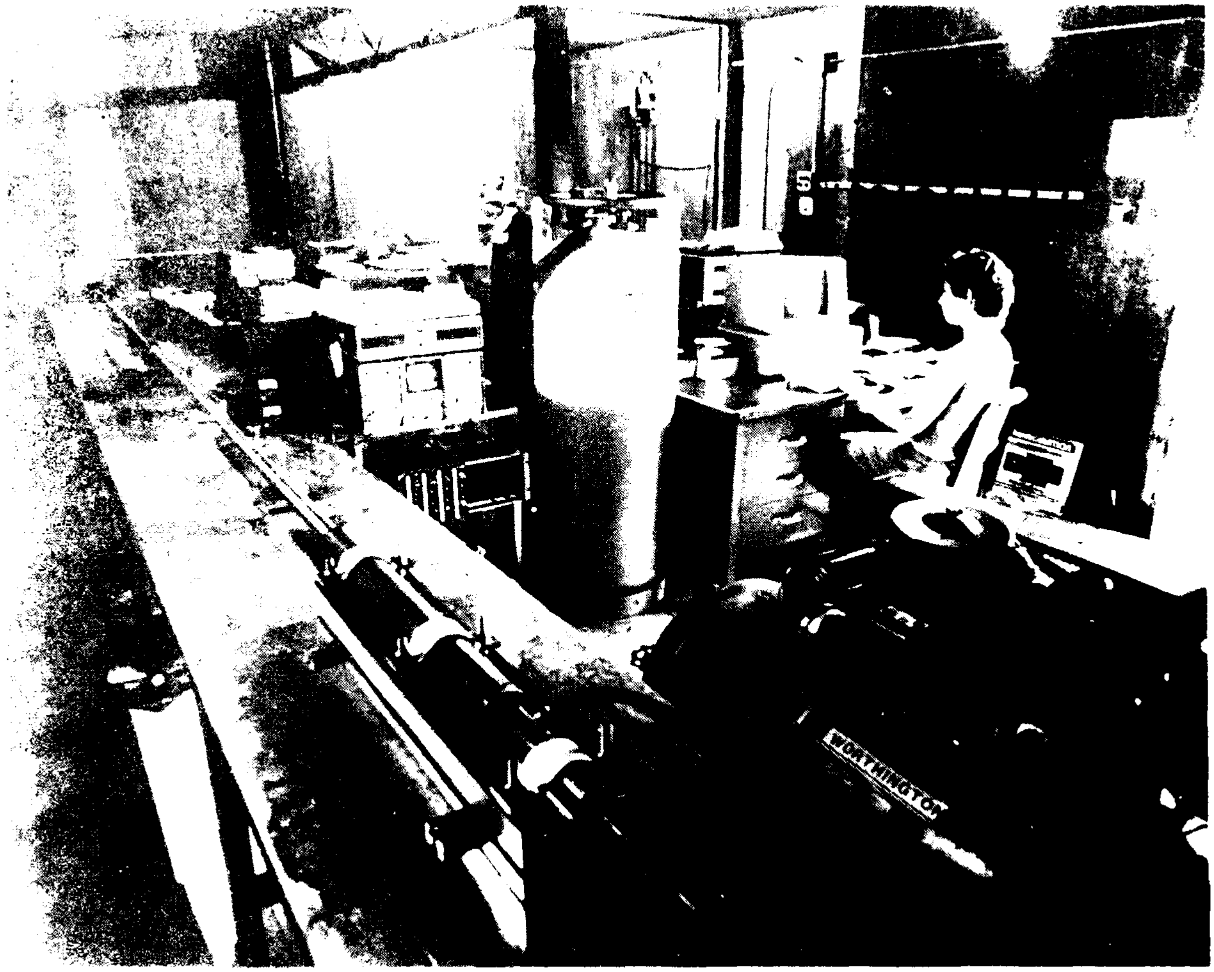

[illegible] Hopkinson pressure bar (HPB) apparatus and systems.

[illegible] measurement system. The following sections describe [illegible] system.

[illegible] consists of a reservoir with a quick- [illegible] r, striker, incident bar, transmitter [illegible]

[illegible] charged to the [illegible] firing, this air is [illegible] air behind [illegible]

the bars must be properly aligned. Proper alignment is also important to ensure that minimum bending waves are generated. Otherwise these waves are sensed by the strain gauges and distort the true uniaxial compression/tension signals. Each bar is guided through three support blocks. The support blocks and the launch cylinder are mounted on a long rigid table. Locations of the blocks and the impactor are adjustable to ensure adequate alignment during test. To reduce dispersion of the stress waves through the support members, the support blocks were specially designed with low-friction ball bearings (Fig. 4). Adjustments are provided on each individual block so that the striker, incident bar, specimen, and transmitter bar are all in alignment.

The striker, the incident bar, and the transmitter bar are made of the same material -- 303 stainless steel. The stainless steel bars were chosen for their noncorrosive characteristics. On impact the stress developed in the bar should be held below its yield stress [67,000 lb/in.^{2} (462 MPa)]. To limit the stress level to 50% of the yield stress, it was calculated that the striker velocity should not exceed 38 ft/s (11.6 m/s). Calculat-

Figure 4. HPB apparatus low-friction support.

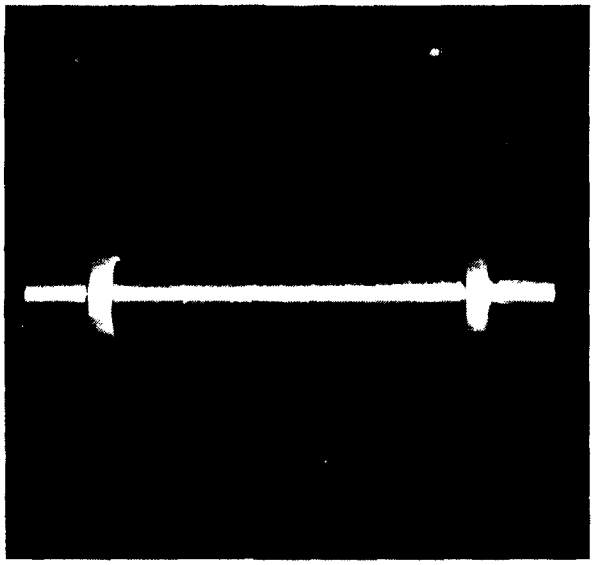

Figure 5. HPB apparatus striker.

ing the kinetics of the striker motion shows that at 100 lb/in.^{2} (689 kPa) pressure a 2-in. (51-mm) stroke is sufficient to reach this velocity.

The striker is 12 in. (305 mm) long and has the same diameter as the incident bar and the transmitter bar [1.5 in. (38 mm)]. Both the incident bar and the transmitter bar are 8 ft (2438 mm) long and have ends machined normal to the bar axis. The striker (Fig. 5) end is rounded with a spherical radius of 12 in. (305 mm) to minimize any misalignment between the striker and the incident bar.

To cause the striker to impact, an 8.5 ft^3 (0.24 m^3) compressed-air gas reservoir is first charged to the required pressure. This has been calibrated to give the desired stress level in the incident bar. Figure 6a shows the air pressure and the corresponding incident stress level data. A quick-operating solenoid valve is then activated to allow the compressed air to drive the striker, which impacts the incident bar. Figure 6b shows the repeatability of the stress wave forms with six separate impacts.

The striker itself is housed in a launch cylinder. The striker bearing surface and the cylinder inside surface form a close fit, with a 0.003-in.-(0.08-mm-)diameter clearance between the striker and the cylinder. This minimizes air leakage and provides guidance for the striker. A 0.25-in.-(6.4-mm-)diameter rod connected to the rear of the striker bar protrudes from the launch cylinder and provides a convenient means to locate the

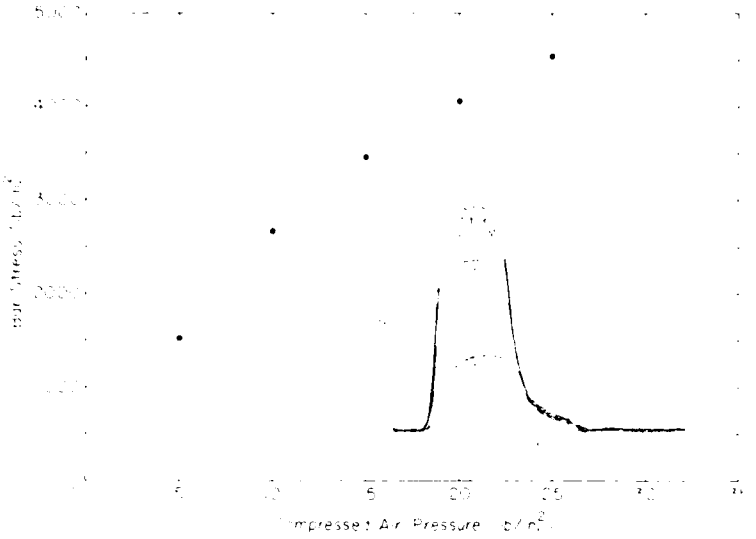

a. At various air-pressure levels used for driving the striker.

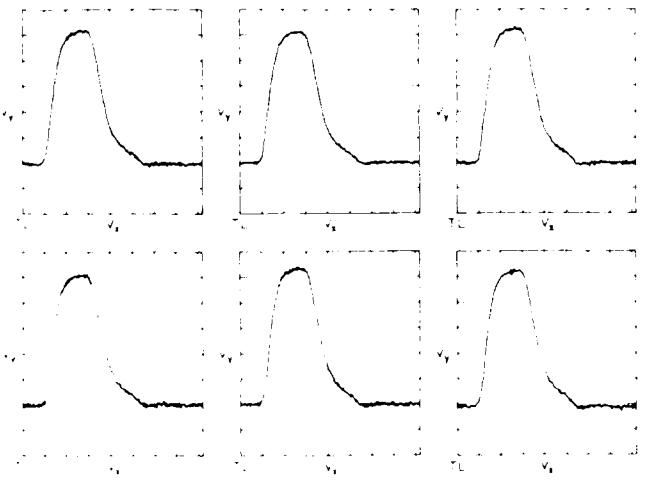

b. Repeatability of the pulses under six separate striker impacts at 20 lb/in.^{2}

Figure 6. Stress wave pulse forms.

striker inside the launch cylinder and adjust the stroke length. The air in front of the striker is vented to atmosphere through two 0.75-in.-(19-mm-)diameter holes in the front part of the launch cylinder. In its current configuration no attempt has been made to measure the velocity of the striker at impact. This is considered a redundant measurement because the electric strain gauging is available to measure accurately the stress level in the incident bar directly. The inside surface of the launch

cylinder is honed to reduce friction and wear. To reduce friction further, the striker bearings are made of Teflon.

The specimen is located between the incident bar and the transmitter bar. A small amount of preloading is necessary to hold the cylindrical specimen in position between the two bars. This is achieved with two rubber bands tensioning the two bars to close on the specimen. In addition, two Teflon collars mate the ends of the specimen to both bars. Each collar is slit lengthwise to allow a modest flexibility in diametrical expansion when required for mounting the specimen.

The striker together with the incident bar, transmitter bar, and the shock absorbing device constitute a set to test material at stresses less than 33,500 lb/in.^{2} (231 MPa).

The specimen materials tested to date are brass, Teflon, and polycrystalline ice. The next section describes the results of testing an ice sample.

The ice specimens were prepared in molds by using snow particles of sizes 0.07 to 0.03 in. (1.78 to 0.833 mm). The mold used to prepare the samples is shown in Figure 7. It was first lubricated and tempered at 10°F

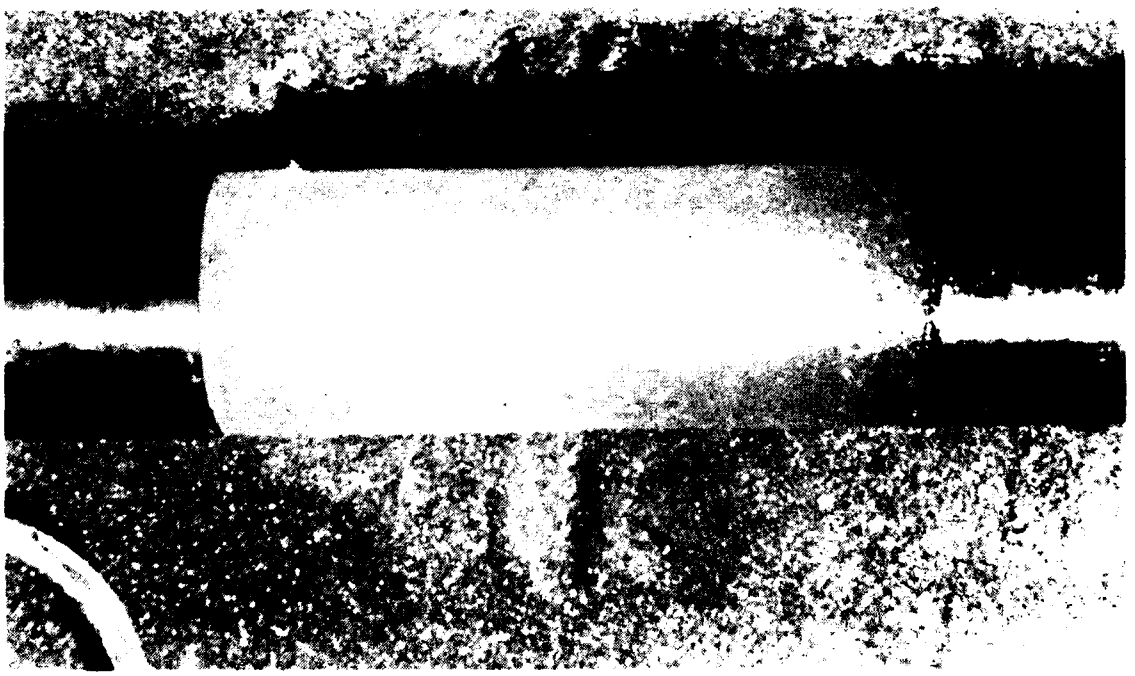

Figure 7. Polycrystalline ice sample mounted on the HPB apparatus for tests.

(-12°C). Then, before adding and tamping the prepared snow in the three chambers, the system was tempered again at 0°F (-18°C). A distilled, de-aired water supply was gravity-fed through the bottom end caps, and the slight overflow was drained through holes in the top end caps to remove any trapped air. With the water still slowly circulating, the mold was returned to 10°F (-12°C) for freezing. A Styrofoam insulation cap was applied to the top of the mold to promote initial ice growth from the bottom of the mold and additional air escape at the top.

After the specimens were frozen, they were tempered several minutes at 40°F (4.4°C) to free the ice from the mold. After they were ejected, each specimen was wrapped in cellophane and stored at 10°F (-12°C).

Specimen Cooling System

To keep the test specimens cold during the impact test, the specimen and the mating ends of both bars are enclosed in two copper-coiled enclosures through which cooled nitrogen gas is circulated. The nitrogen gas is cooled by circulating it through a liquid nitrogen bath. The details of the cooling system are shown in Figure 8. The coils themselves are enclosed in a Styrofoam container. The specimen temperature is monitored with a thermocouple.

Temperature is controlled by the level of immersion of the cooling coil in the liquid nitrogen and the flow rate of the nitrogen gas through the coils. With this arrangement a stable temperature as low as -90°F (-68°C) can be achieved. In the current design configuration the N_2 gas flow is branched to two specimen-cooling coils. Continuous operation of the coils also chills the ends of the Hopkinson bars, permitting rapid restabilization of specimen temperatures.

Stress Measurement System

In performing the experiments it is necessary to record the complete profiles of the incident stress wave pulse and reflected stress wave pulse in the incident bar and the transmitted wave pulse in the transmitter bar. For this purpose foil strain gauges were bonded on both the incident and transmitter bars at the midpoint of each length. The positions of the gauges and the lengths of the bars were so selected that the stress wave signals could be recorded for their entire duration without interruptions caused by wave reflections from the ends. Two active strain gauges were mounted on each bar, one diametrically opposite the other to cancel bending wave strain, if any is produced because of misalignment.

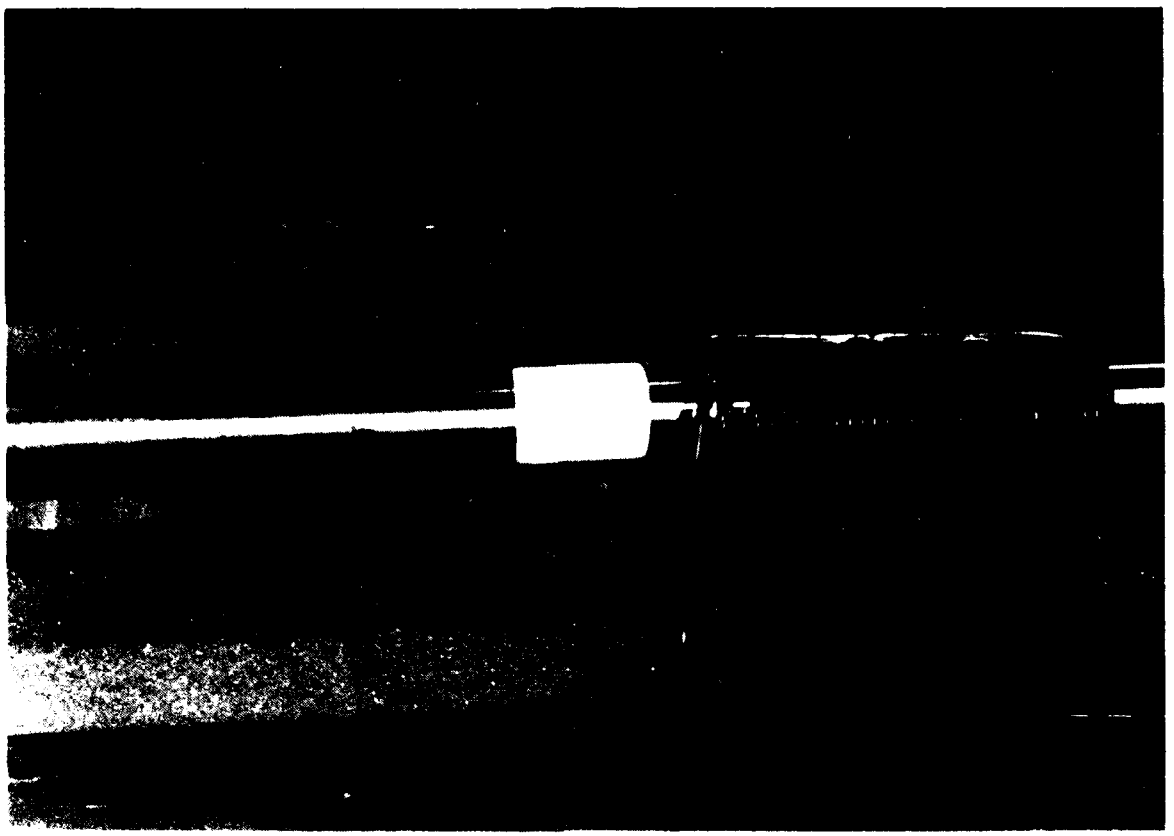

Figure 8. Cooling system: specimen-cooling coil circulating cooled N_2 gas.

The schematic for the electronic circuitry is shown in Figure 9. The strain gauge outputs after preamplification are fed to a Model 4562 plug-in unit of a Nicolet 4094A Digital Oscilloscope. Channel A is used for recording the incident and reflected waveform and channel B for the transmitted wave. The waveforms are sampled at 0.5-μs intervals and digitized with 12-bit resolution. The scope has the capability to expand the wave forms after recording. It can store and recall data from a floppy disk. The scope is compatible with the Hewlett Packard Model 7470A X-Y plotter for plotting the displayed waveforms on paper.

An on-line data acquisition and analysis system has been assembled using a PC<>488 interface board (manufactured by Capital Equipment Corp.) in an IBM PC/AT computer. Suitable software has been developed to transmit the stored or recorded data from the scope to the computer for analysis.

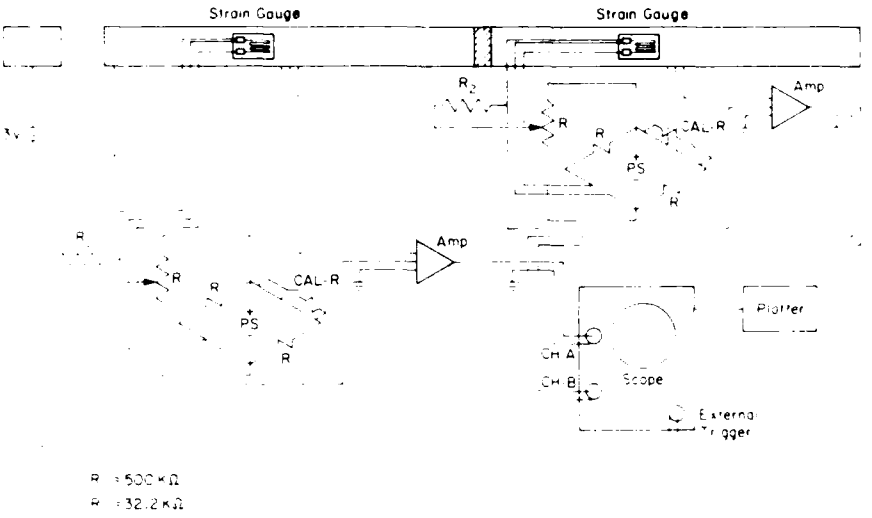

Figure 9. Stress pulse waveforms recording electronic circuit schematic.

In initiating the test the sweeps were triggered by electrical contact between the striker and the incident bar. Figure 9 includes the schematic of the triggering circuit.

The system was calibrated dynamically by stress wave recording induced in both bars butted together without a specimen. Figure 10 shows these two waveforms. Note that on the first trace the reflected wave from the butted surface is only 4% of the total energy transmitted to the second bar. In

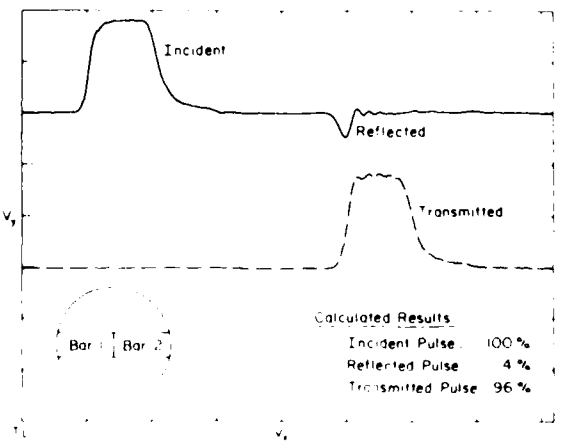

Figure 10. Incident, reflected, and transmitted stress pulse wave from a single impact on the bars belted to each other.

addition, calibration resistors across one arm of the strain gauge bridge were used to produce simulated strain. The details of the instrumentation are given in Appendix B.

WAVEFORM ANALYSIS

Before performing the analysis, the three waveforms stored in the two sweeps are first transferred to the IBM PC/AT using the computer program HOPP specifically written for the data transfer from the Nicolet oscilloscope.

When the digitized data transfer is complete, the program will reconstitute the waveforms (incident, reflected, and transmitted) and superimpose them on a common time base for viewing on the CRT display and ensuring there is no flaw in the data transfer. The details of the computer program and data transfer technique have been documented separately (Dutta 1986). Figure 11 shows the data before transmission as photographed from

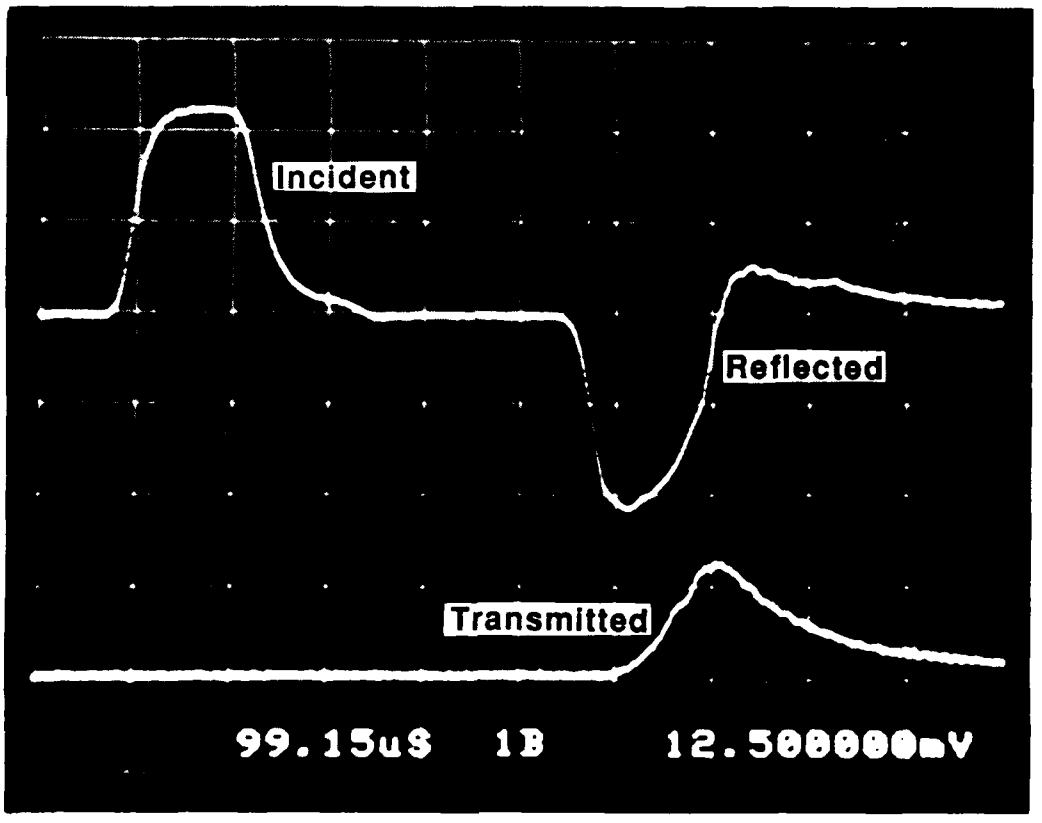

Figure 11. Stress pulse waveform data on oscilloscope.

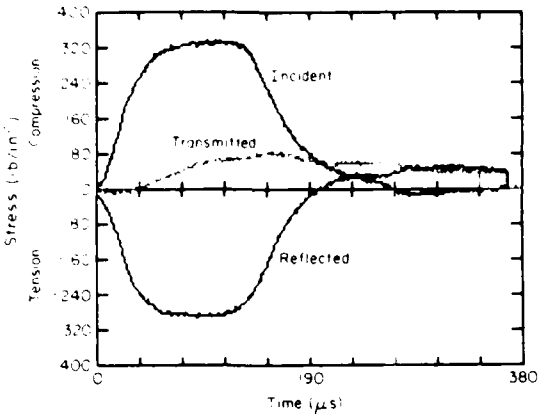

Figure 12. Incident, reflected, and transmitted stress pulse waves reconstituted on the computer screen.

the oscilloscope screen. Figure 12 shows the hardcopy printout after the data are reconstructed by the computer program. The HOPP program then continues to analyze these waveforms using eq 4, 5, and 6 to produce the time-variant data on specimen average strain, specimen stress, and strain rate. The stress-strain data is displayed on the CRT screen and can also be printed out on a printer. The plot of the strain rate vs strain is also displayed on the CRT screen and again can be printed out. Figure 13 shows the plot of the stress-strain curve of the specimen during passage of the stress wave and Figure 14 shows strain rate vs strain. If desired, a point-by-point data analysis report at specified time intervals in tabulated format can also be printed out.

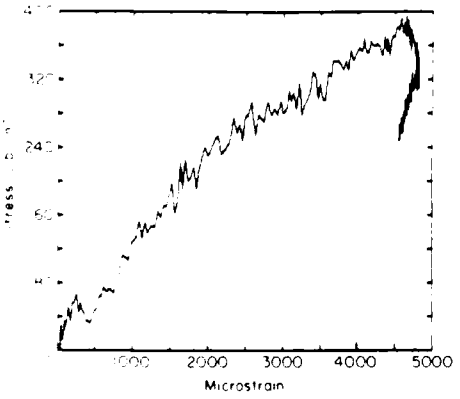

Figure 13. Dynamic stress-strain relationship of an ice sample computed from the stress pulse waveforms.

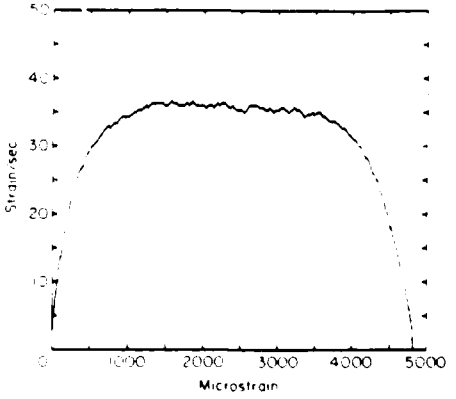

Figure 14. Strain rate vs. strain of an ice sample during passage of the stress wave.

GENERAL COMMENTS

The Hopkinson bar apparatus with its associated data recording and analysis equipment is a convenient means to perform a quick evaluation of materials under high strain rate loading. However, it must be recognized that the approach is an indirect one, and the strain rates that occur during the test are primarily a function of the material's own constitutive property. Moreover, two important assumptions are made in the analysis that influence the results: 1) nondispersivity of the elastic waves in the bar and 2) the absence of radial inertia.

For these reasons the split Hopkinson bar has been the subject of an extensive analytical study to evaluate the validity of the results obtained from its tests. Davies (1948) was the first to examine critically the effects of wave dispersion in the Hopkinson bar; he concluded that the dispersion effects can disguise the stress change that happens within any 1-μs interval. Inertial effects were studied by Davies and Hunter (1963), who recommended that to minimize error due to inertial effects and interfacial friction the optimum geometry for the specimens should be a/h = 1.15 where a is the radius and h is the thickness of the specimen. Interfacial friction problems were studied in great depth by Bertholf and Karnes (1975), whose results show that lubricated interfaces have the minimum error.

Another important consideration in performing the Hopkinson bar test on specimens at other than ambient temperature is the influence of the temperature gradient along the bar. Malvern (1984), as reported by Zukas et al. (1982), has considered this problem. His analysis is based on the assumption that the modulus E is linearly dependent on temperature.

Assuming that the temperature gradient is linear, a more straightforward derivation of the correction factor is possible. The relation between the stress near the sample (σ_s) and the stress measured at the gauge station (σ_g) can be obtained by considering the general relationship (refer to Zukas 1982)

$$\frac{\sigma_g}{\sigma_s} = \left(\frac{E_g}{E_s}\right)^{0.5} \tag{7}$$

where E_g is the modulus of elasticity of the bar material at the gauge station at ambient temperature T_a, and E_s is the modulus of elasticity

of the bar material near the specimen at test temperature T_s. For the CRREL Hopkinson bar made of AISI 303 stainless steel, E_g at 0°F (-18°C) = 29.4×10^6 lb/in.^{2} (202.6 GPa) and $E_s = 28.3 \times 10^6$ (195.0 GPa) at -300°F (-184°C). Using these values, the error due to a 0 to -300°F (-18 to -184°C) temperature differential will be approximately 2%.

In interpreting the Hopkinson test bar data it is also important to take into consideration the stress wave reflections, stress nonuniformity, and large variation of strain, especially during the initial and final portions of the test. The stress-strain data are thus valid only after some degree of uniformity in stress and strain is achieved. Figure 14 shows that the strain rate changed rapidly till the strain was established at about 36 strains/s. Once strain rate uniformity is established, the dynamic stress-strain characteristic data are more valid.

A series of tests has been conducted using ice samples and a few other engineering materials. These data are the subject of another report now in preparation. However, it has been generally observed that at the low stress level in a semibrittle material such as ice, the stress-strain curve is smoother than that obtained with higher stress level loading (Fig. 15). At the low stress level only a few cracks were induced in the sample, whereas at a high stress level impact the specimen shattered (Fig. 16). Multiple reflections of the stress waves within the sample during the fracturing may have contributed to the sawtooth characteristic of the stress-strain curve for high-level stress loading.

The heart of the system, which gives an indirect measurement of the dynamic constitutive relationship, is the correct recording of the waves in the pressure bars. The three stress waveforms -- $\sigma_i(t)$, $\sigma_r(t)$, and $\sigma_t(t)$ -- form the very basis of this analysis. Since $\sigma_i(t)$ is recorded earlier and both $\sigma_r(t)$ and $\sigma_t(t)$ are recorded later than they occur at the interface, the recorded stress waveforms must be appropriately shifted in time before they are combined as in eq 4, 5, and 6. The use of a digital oscilloscope and the data transfer and analysis techniques now developed allow the incident bar/specimen interface and transmitter bar/specimen interface displacement to be determined accurately -- thus the average strain in the specimen can be computed by taking the arithmetic mean of the two interface displacements. The deviation from the average displacement is estimated as half the difference between the two.

This procedure has not been used much in the past. Most of the data in the literature were obtained before automated data recording and analysis. The usual procedure has been to assume that the two interface displacements are equal, neglecting strain variation along the length of the specimen. For short specimens, where strain uniformity could be achieved rapidly and the stress pulse is of long duration, this assumption may not lead to any great error, but the current design allows a better averaging technique for comparatively longer specimens.

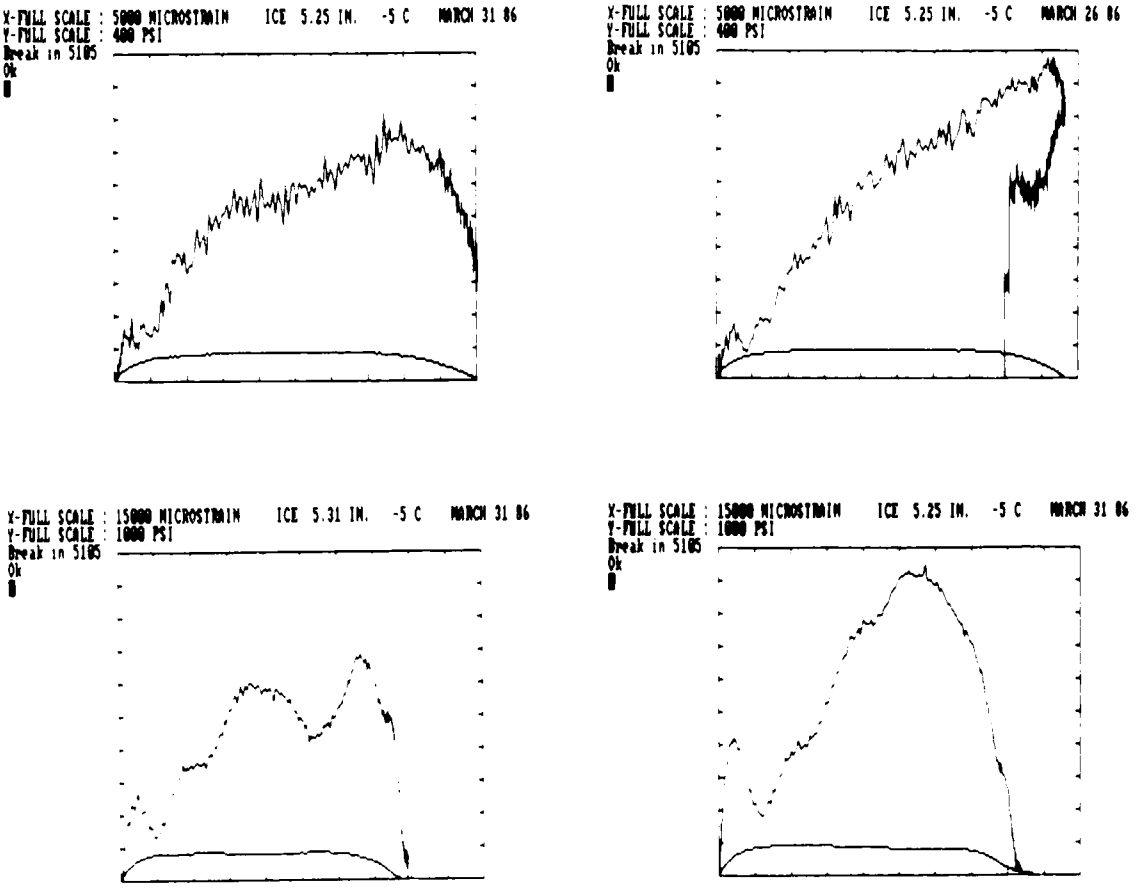

Figure 15 Typical dynamic stress-strain data from tests of polycrystalline ice samples.

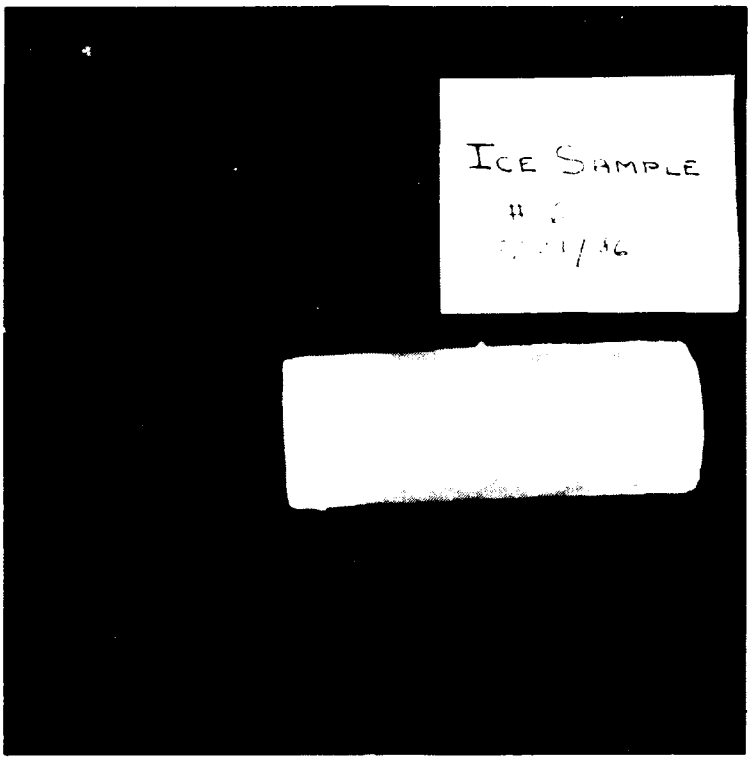

a. Low stress level (400 lb/in.^{2}) sample.

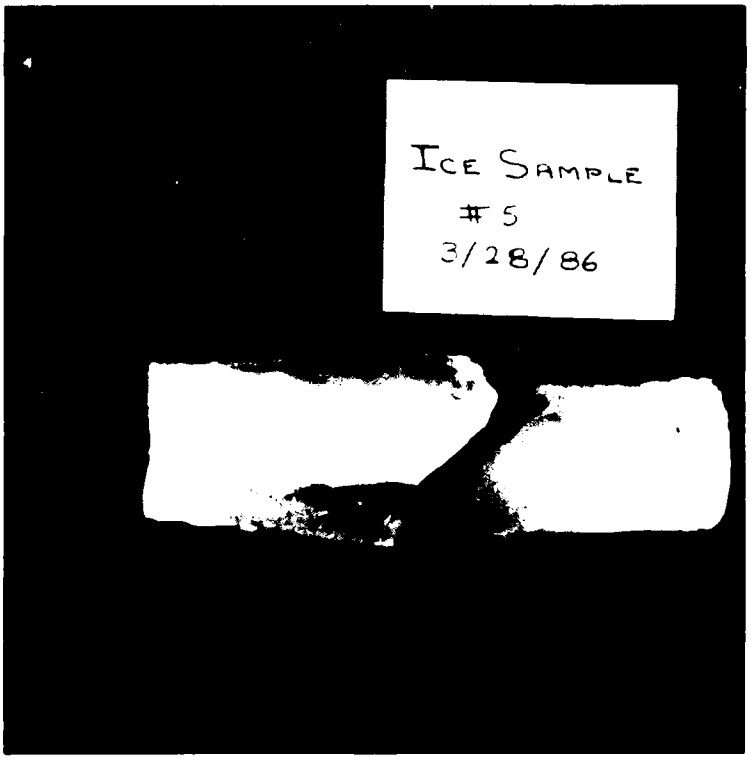

b. High stress level (1000 lb/in.^{2}) sample.

Figure 16. Ice samples after test.

LITERATURE CITED

Berthholf, L.D. and Karnes, C.H. (1975) Two-dimensional analysis of the split Hopkinson Pressure Bar System. Journal of Mech. Physical Solids, 23:1-19.

Christman, D.R., W.M. Isbell, S.G. Babcock, A.R. McMillan and S.J. Green (1971) Measurement of dynamic properties of materials. Report No. DASA 2501-2, MSL 70-23, vol. II, Arlington, Va.

Davies, R.M. (1948) A critical study of the Hopkinson Pressure Bar. Phil. Transactions of the Royal Society, London, Series A, 240: 375.

Davies, E.D.H. and Hunter, S.C. (1963) The dynamic compression testing of solids by the method of the Split Hopkinson Pressure Bar. Journal of Mech. Physical Solids, 11: 155.

Duffy, J., J.D. Campbell and R.H. Hawley (1971) On the use of a torsional Split Hopkinson Bar to study rate effects in 1100-0 aluminum. Journal of Applied Mechanics, Transactions of the ASME, 38: 83-91.

Dutta, P.K. (1986) Hopkinson pressure bar data acquisition and analysis methods. CRREL Technical Note.

Harding, J. (1983) Tensile impact testing of fiber-reinforced composites. 20th Annual Meeting, Society of Engineering Science, University of Delaware, Newark, Delaware.

Harding, J., E.O. Wood and J.D. Campbell (1960) Tensile testing of materials at impact rates of strain. Journal of Mechanical Engineering Science, 2: 88.

Hauser, F.E. (1966) Techniques for measuring stress-strain relations at high strain rates. Experimental Mechanics, 6: 395.

Hopkinson, B. (1914) A method of measuring the pressure produced in the detonation of high explosives or by the impact of bullets. Philosophical Transactions of the Royal Society, London, Series A, 213(10): 437-456.

Klepaczko, J. (1980) In Mechanical properties at high rates of strain. (J. Harding, Ed.) London: Institute of Physics, p. 201.

Kolsky, H. (1949) An investigation of the mechanical properties of materials at very high rates of loading. Proceedings of the Physical Society, 62-B:676-700.

Kolsky, H. (1953) Stress waves in solids. Oxford: Clarendon Press.

Lindholm, U.S. (1964) Some experiments with the Split Hopkinson Pressure Bar. Journal of Mechanical Physical Solids, 12: 317-335.

Lindholm, U.S. and Yeakley, L.M. (1968) High strain rate testing: Tension and compression. Experimental Mechanics, 8(1): 1-9.

Malvern, L.E. (1984) Experimental and theoretical approaches to characterization of material behavior at high strain rates of deformation, in Mechanical Properties of High Rates of Strain (J. Harding, Ed.) London: Institute of Physics, pp. 1-17.

Nicholas, T. (1975) Air Force Materials Laboratory Report AFML-TR-75-54. Ohio: Wright Patterson AFB.

Nicholas, T. (1981) Tensile testing of materials at high rates of strain. Experimental Mechanics, 21(5): 177-185.

Ross, C.A., W.H. Cook and L.L. Wilson (1984) Dynamic tensile tests of composite materials using a Split Hopkinson Pressure Bar. Experimental Techniques, 30: 30-33.

Stein, P. (1967) Some properties of input conditioning circuits for Wheatstone Bridge-based transducers. Publication no. 12. Tempe, Arizona: Measurement Engineering Laboratory, College of Engineering Sciences, Arizona State University.

Zukas, J.A., T. Nicholas, H.F. Swift, L.B. Greszczuk and D.R. Curran (1982) Impact dynamics. New York: John Wiley and Sons.

APPENDIX A. THEORY OF THE APPARATUS

Elementary plane wave propagation theory (Zukas et al. 1982, Malvern 1984).

In the one-dimensional propagation of a stress wave through a solid bar the following assumptions are made:

1) A plane cross section remains plane as the wave propagates along the longitudinal axis.
2) Stress distribution is uniform across the section of the bar.
3) Radial inertia can be neglected.

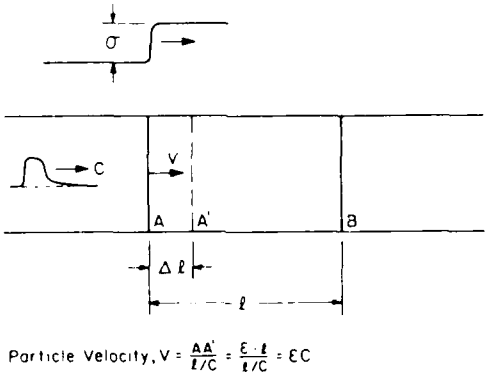

Figure A1. Elementary uniaxial plane wave propagation.

In Figure A1 consider an element AB having a length l on this bar. A stress pulse of amplitude σ (and strain $\varepsilon = \sigma/E$) traveling with a wave velocity c arrives at plane A at the instant t = 0. It arrives at plane B after a time l/c. During this time the element AB is under compression σ, therefore plane A moves to A' such that

AA' = deformation = ε l .

The velocity of A (called the particle velocity V) is then given by:

$$V = \frac{AA'}{l/c} = \frac{\varepsilon\, l}{l/c} = \varepsilon c \qquad \text{(A1)}$$

However, it is well known that in an elastic medium of density, ρ, the propagation of a longitudinal wave, is given by

$$c = (E/\rho)^{0.5} \qquad \text{(A2)}$$

or

$$E = c^2\rho$$

Since $\sigma = E\,\varepsilon$ from eq A1 and A2

$$\sigma = c^2\rho\cdot\frac{V}{c} = \rho cV \tag{A3}$$

the displacement U of the particle at any time t is given by

$$U = \int_0^t V(t)dt = \frac{1}{\rho c}\int_0^t \sigma(t)dt \tag{A4}$$

Split Hopkinson bar wave mechanics

Consider x and y as the ends of two bars of the same diameter and material. Any wave in which the particle moves to the right is assumed to move in a positive (+) direction, and one that moves to the left assumes a negative (-) direction. Thus, a compression wave that propagates to the right has the particle velocity in the positive direction, and a tensile wave that moves to the left has a positive particle velocity.

A compressive stress wave pulse arriving at the x-y boundary is partially transmitted and also partially reflected.

If $\sigma_i(t)$ = stress wave incident to the sample sandwiched between the two bar edges x and y, then displacement U_i of the x face, due to the incident stress wave pulse $\sigma_i(t)$, is given by

$$U_i = \frac{1}{\rho c}\int_0^t \sigma_i(t)dt$$

and displacement U_r of the x face due to the reflected stress wave pulse $\sigma_r(t)$ is

$$U_r = \frac{1}{\rho c}\int_0^t \sigma_r(t)dt$$

As the reflected wave travels in the direction opposite to the incident wave, the total displacement of the x face is given by

$$U_i - U_r = \frac{1}{\rho c}\int_0^t [\sigma_i(t) - \sigma_r(t)]dt\ . \tag{A5}$$

Similarly, displacement of the y face due to the transmitted stress wave pulse $\sigma_t(t)$ is given by

$$U_t = \frac{1}{\rho c}\int_0^t \sigma_t(t)dt \tag{A6}$$

Therefore, total deformation U_T of the sample due to passage of the stress wave pulse through it is

$$U_T = U_i - U_r - U_t$$

or

$$U_T = \frac{1}{\rho c} \int_0^t [\sigma_i(t) - \sigma_r(t) - \sigma_t(t)]dt \ . \qquad (A7)$$

Note that to obtain U_t from eq A6, $\sigma_t(t)$ should be measured at the same instant that $\sigma_i(t)$ and $\sigma_r(t)$ are measured. If Δt = time required for the wave to propagate from face x to y and $\sigma_r(t)$ is measured at time T after start of the sweep, then $\sigma_t(t)$ should be measured at time T + Δt. If L_s = length of the sample, then the instantaneous sample strain $\varepsilon_s(t)$ is given by

$$\varepsilon_s(t) = \frac{U_T}{L_s} = \frac{1}{\rho c L_s} \int_0^t [\sigma_i(t) - \sigma_r(t) - \sigma_t(t)]dt \qquad (A8)$$

Therefore the sample strain rate ($\dot{\varepsilon}_s$) can be obtained by differentiating the above integral expression ε_s with respect to time, i.e. $d\varepsilon_s(t)/dt$ is given by

$$\dot{\varepsilon}_s = \frac{1}{\rho c L_s} [\sigma_i(t) - \sigma_r(t) - \sigma_t(t)] \ . \qquad (A9)$$

Sample stress at interface x is given by the algebraic sum of the incident stress $\sigma_i(t)$ and the reflected stress $\sigma_r(t)$; i.e.

the stress at interface x, $\sigma_x(t) = \sigma_i(t) + \sigma_r(t)$ (A9.1)

the stress at interface y, $\sigma_y(t) = \sigma_t(t)$ (A9.2)

The average sample stress of $\sigma_s(t)$ is given by the mean of the stress at the x and y interfaces, i.e.

$$\sigma_s(t) = \frac{1}{2} [\sigma_i(t) + \sigma_r(t) + \sigma_t(t)] \qquad (A10)$$

By using eq A8, A9, and A10 the complete stress-strain wave and the strain rate loading in the HPB set-up can be determined.

Short specimens

If the length of the sample is short, then the stress at interface x can be assumed to be same as the stress at interface y, i.e. from eq A9.1 and A9.2

$$\sigma_t(t) = \sigma_i(t) + \sigma_r(t)$$

or

$$-\sigma_r(t) = \sigma_i(t) - \sigma_t(t) \ . \qquad \text{(A11)}$$

Substituting the above in eq A8,

$$\varepsilon_s(t) = \frac{-1}{\rho c L_s} \int_0^t 2\sigma_r(t)dt \ . \qquad \text{(A12)}$$

Again, $\sigma_r(t) = E\ \varepsilon_r(t) = c^2\rho\varepsilon_r(t)$

and $$\varepsilon_s(t) = \frac{-2c^2\rho}{\rho c L_s} \int_0^t \varepsilon_r(t)dt \ ;$$

therefore $$\varepsilon_s(t) = \frac{-2c}{L_s} \int_0^t \varepsilon_r(t)dt \qquad \text{(A13)}$$

and strain rate

$$\frac{d\varepsilon_s(t)}{dt} = \dot{\varepsilon}_s = \frac{-2c}{L_s}\ \varepsilon_r(t) \ . \qquad \text{(A14)}$$

Again substituting eq A11 in eq A10, the sample stress for a short sample is given by

$$\sigma_s(t) = \frac{1}{2}\ [2\sigma_t(t)] = \sigma_t(t) \ , \qquad \text{(A15)}$$

therefore

$$\sigma_s(t) = E_b\varepsilon_t(t) \ . \qquad \text{(A16)}$$

APPENDIX B. INSTRUMENTATION OF THE HPB APPARATUS

Strain was measured at the midpoint on each half of the split Hopkinson bar. Two 0.125-in. (3.18-mm) long, 350-ohm strain gauges, compensated for stainless steel, were attached at each location. One was aligned diametrically opposite the other for bending moment compensation. The gauges, Type CEA-09-125 UR-350, were bonded with AE-10 epoxy and cured at room temperature according to accepted procedures. The gauge dimensions (0.125 x 0.60 in.) were chosen so strain averaging would occur over only a small physical area of the bar.

The gauges were connected into a bridge configuration with the three-wire technique. Each gauge cable was individually shielded and the gauge was wired into opposing sides of a two-active-arm, four-arm bridge. This configuration offers twice the voltage output of a two-gauge, one-active-arm, four-arm bridge with less nonlinearity and only a minimal loss of bending compensation. Micro Measurement M Coat D was used over the completed gauge installation for moisture protection. Each gauge was connected to the bridge completion and balance circuit by 15 ft (4.6 m) of Belden 8723 cable where the four-arm bridge was completed with 350-ohm fixed resistors.

Bridge balance was achieved with the 500-kohm potentiometer, as shown in Figure 9 of the text. The balance circuit was designed as described by Stein (1967). Bridge excitation was set at 15V and was provided by the Hewlett Packard HP 6218B power supply. Each bridge had its own independent power source.

Both amplifiers were set on a gain of ten, which provided a corresponding bandwidth of 100 kHz with 120 dB of common mode rejection at their differential inputs. The output of each amplifier was single-ended and connected into the positive input terminal of each scope channel. Data was recorded on the ±100 mV settings and digitized at the rate of 0.5 μs per point, giving a record length of about 4 ms. Two channels on the scope were used: channel 1 recorded incident and reflected strain and channel 2 recorded the transmitted strain. The oscilloscope trace was triggered when the hammer contacted the first bar of the split Hopkinson bar. This contact applied a 3V battery voltage directly to the external trigger input of the scope.

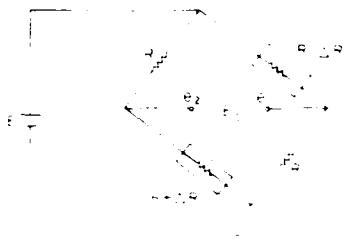

Figure B1. Bridge configuration for bending wave effort analysis.

Figure B2. Bridge configuration for shunt calibration.

The bridge configuration used for recording the strains in the bars is shown in Figure B1. In this model the strain generated by bending will have an insignificant effect on the longitudinal strains computed from E_{out}.

For example, in the bending configuration the change of strain ΔR will be positive in one gauge and negative in the opposite gauge, so that

$$E_{out} = e_1 - e_2 = \frac{ER}{2R - \Delta R} - \frac{E(R+\Delta R)}{2R + \Delta R},$$

which on simplification gives

$$E_{out} = E \cdot \frac{\Delta R^2}{4R^2 - \Delta R^2} \qquad (B1)$$

Since ΔR has a very small value compared to R, E_{out} for bending is negligibly small.

Calibration was performed with the usual gauge shunt technique. When shunted with the 349,650-ohm resistor shown in Figure B2, each active gauge gave the equivalent of 250 microstrain at the oscilloscope input, as shown below:

$$R_{AD} = \frac{R_1 R_S}{R + R_S} = \frac{(350)(349650)}{350 + 349650} \approx 349{,}650 \text{ ohm}$$

$$e_2 = \frac{E_1 R_{AD}}{R + R_S} = \frac{340650\ E}{350 + 349650} = 0.49975\ E$$

$$e_1 = \frac{E}{2}.$$

Therefore $E_0 = e_2 - e_1 = 0.00025\ E$ or $E_0/E = 0.00025$. But

$$E_0/E = \frac{\text{gauge factor x strain}}{2},$$

therefore

$$\text{strain} = \frac{0.00025 \times 2}{\text{gauge factor}}$$

Assuming the gauge factor is 2, strain = 0.00025 = 250 microstrain.

External noise pickup was kept to an acceptable level with careful equipment layout. The metal table supporting the split Hopkinson bar was tied to a handy electrical conduit and this became the electrical common point. As mentioned earlier, the gauge cables were individually shielded and tied at the far end to the electrical common as were all enclosures and shields. Bridge configuration and excitation were chosen to give a high electrical output, and the dc amplifier provided 120 dB of common mode rejection from dc to 60 Hz.

The scope was capable of outputting the digitized data directly to a plotter although most data was stored on floppy disks and later transmitted to a computer for further analysis.

Table B1. Instrumentation components.

Qty.	Description	Manufacturer	Model No.
4	Strain gauge	Micro Measurements	CEA-09-125 UR-350
4	Calibration resistors	Micro Measurements	W-349650-02
4	Bridge completing resistors	Micro Measurements	S-350-01
1	Bridge completion and balance unit	In-house	--
2	Power supply	Hewlett Packard	HP 6218B
1	Graphics plotter	Hewlett Packard	HP 7470A
1	Interface board	Capital Equip. Co.	PC<>488
1	Digital oscilloscope with dual amplifiers and dual disk drives	Nicolet Instrument Co.	4099A 4562 XF44
1	External scope trigger (3V battery)	Union Carbide Corp.	W-356
	Gauge epoxy	Micro Measurements	AE-10
	Gauge cable	Belden	8723

END
DATE
FILMED
5-88
DTIC